We are IntechOpen, the world's leading publisher of Open Access books Built by scientists, for scientists

4,800
Open access books available

122,000
International authors and editors

135M
Downloads

Our authors are among the

154
Countries delivered to

TOP 1%
most cited scientists

12.2%
Contributors from top 500 universities

CLARIVATE ANALYTICS BOOK CITATION INDEX INDEXED

WEB OF SCIENCE™

Selection of our books indexed in the Book Citation Index in Web of Science™ Core Collection (BKCI)

Interested in publishing with us?
Contact book.department@intechopen.com

Numbers displayed above are based on latest data collected.
For more information visit www.intechopen.com

16

Analysis and Modelling of Surface Acoustic Wave Chemical Vapour Sensors

Marija Hribšek and Dejan Tošić
Institute Goša Belgrade, University of Belgrade
Serbia

1. Introduction

Surface Acoustic Wave (SAW) sensors demonstrate superior selectivity for the detection of chemical agents. Due to their solid state design and fabrication, compatible with other modern technologies such as MIC (microwave integrated circuits), MEMS (micro-electro-mechanical-systems), CMOS, CCD (charge coupled devices) and integrated optic devices, SAW chemical sensors are extremely reliable. They have compact structure, high sensitivity, small size, outstanding stability, low cost, fast real-time response, passivity, and above all the ability to be incorporated in complex data processing systems. They can be used for *in situ* monitoring and sensing systems [Ho et al., 2003; Wohltjen & Dessy, 1979; Wohltjen, 1984; Comini, 2009] and for wireless sensing and monitoring in harsh environment [Pohl, 2000] including the detection of chemical warfare agents [Data Sheet, 2005] and land mine detection [Kannan et al., 2004]. It is interesting that a SAW-based sensor system is used as a volatile organic contamination monitoring system for the satellite and space vehicle assembly rooms in NASA. SAW sensors can distinguish organophosphates, chlorinated hydrocarbons, ketones, alcohol, aromatic hydrocarbons, saturated hydrocarbons, and water [Ho et al., 2003].

Surface acoustic waves were discovered in 1885 by Lord Rayleigh and are often named after him as Rayleigh waves [Rayleigh, 1885]. A surface acoustic wave is a type of mechanical wave motion which travels along the surface of a solid material, referred to as substrate. The amplitude of the wave decays exponentially with distance from the surface into the substrate, so that the most of the wave energy is confined to within one wavelength from the surface [Farnell, 1977; Martin et al., 1994].

A basic SAW device was originally developed in 1965 [White & Voltmer, 1965] by White and Voltmer when they found out how to launch a SAW in a piezoelectric substrate by an electrical signal. The basic SAW device consists of two interdigital transducers (IDTs) on a piezoelectric substrate such as quartz, Fig. 1.

Each IDT is a reversible transducer made of interleaved metal electrodes, which are used to convert an electrical signal to an acoustic wave and vice versa. An IDT is a bidirectional transducer: it radiates energy equally on both sides of the electrodes. Consequently, theoretical insertion loss introduced by an IDT is at least 6 dB. SAW devices work in the frequency range of 10 MHz to several GHz.

Source: Acoustic Waves, Book edited by: Don W. Dissanayake,
ISBN 978-953-307-111-4, pp. 466, September 2010, Sciyo, Croatia, downloaded from SCIYO.COM

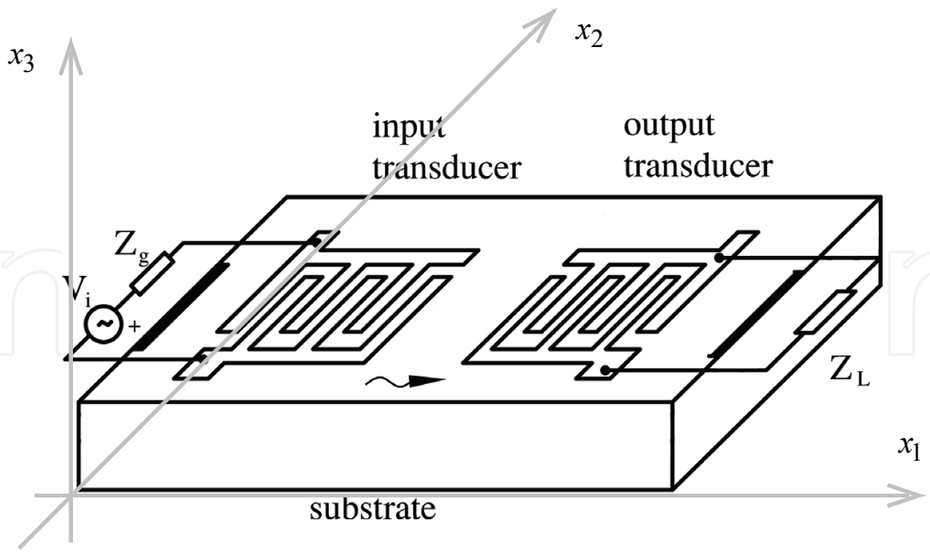

Fig. 1. The basic structure of a SAW device.

A sinusoidal voltage v of frequency f applied to the input IDT forms an electric field which through the piezoelectric effect causes a strain pattern of periodicity $2d$, where d denotes the distance between the centres of the electrodes. If the frequency f is such that $2d$ is close to the surface wave wavelength, a surface wave will be launched in two opposite directions away from the transducer. The surface wave causes the corresponding electric field in the output transducer and thus the voltage at the impedance Z_L. The magnitude of the output signal is the function of the ratio of the signal's wavelength and the distance $2d$. If the distance $2d$ is equal to the wavelength, the magnitude of the output voltage is maximal. The corresponding frequency is then called the centre or synchronous frequency of the device. The magnitude of the output voltage decays as the frequency shifts from the centre frequency. It means that a SAW device is a transversal bandpass filter with constant group delay. Therefore, it is usually called a SAW filter or delay line type of a SAW device. The phase characteristic is a function of the distances between the electrodes and the amplitude characteristic is a function of the electrodes' number and lengths. The width of the electrodes usually equals the width of the inter-electrode gaps giving the maximal conversion of electrical to mechanical signal and vice versa. The minimal electrode width obtained in industry is around 0.3 μm, which determines the highest frequency of around 3 GHz. The commonly used substrate crystals are: quartz, lithium niobate, lithium tantalate, zinc oxide and bismuth germanium oxide. They have different piezoelectric coupling coefficients and temperature sensitivities. The ST quartz is used for the most temperature stable devices. The wave velocity is a function of the substrate material and is in the range of 1500 m/s to 4800 m/s, which is 10^5 times lower than the electromagnetic wave velocity. This enables the construction of a small size delay line of a considerable delay.

In the second type of SAW devices, called SAW resonators, Fig. 2, IDTs are used only as converters of electrical to mechanical signals and vice versa, but the amplitude and phase characteristics are tailored using the reflections of the wave from either metal stripes or grooves of small depths.

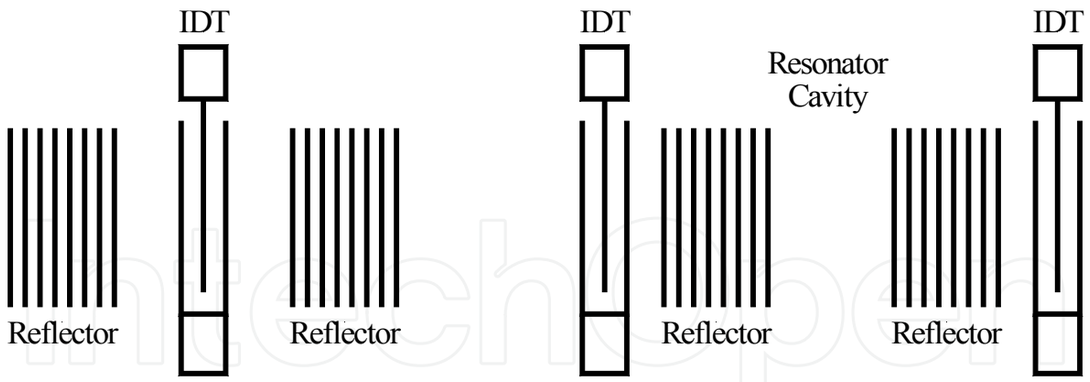

Fig. 2. a) One-port SAW resonator and b) two-port SAW resonator.

SAW resonators are made as one-port or two-port devices. In a one-port SAW resonator only one IDT, placed in the centre of the device, is used for both, input and output, transductions. The input electrical signal connected to IDT, via antenna or directly, forms an acoustical wave in the piezoelectric substrate which travels along the surface on both sides from the transducer. The wave reflects from the reflective array and travels back to the transducer, which transforms it back to the electrical signal. The attenuation of the signal is minimal if the frequency of the input signal matches the resonant frequency of the device. The resonant frequency is determined by the geometries of the transducer and reflectors, the distance between the transducer and the reflectors and the wave velocity. The wave velocity depends upon the substrate type, and the temperature. One-port resonators are used in oscillators. Two-port resonators are used as narrow bandpass filters. The dimensions of resonators are smaller than the delay line filters of the same centre frequency and bandwidth.

Beginning from around year 1970, versatile SAW devices were developed for pulse compression radars, band pass filters for the TV receivers (sets), and radio systems. The rise of mobile radio of the eighties, and particularly cellular telephones, caused an increase in the demand for SAW filters, so that they are now produced in vast number.

In the last three decades SAW devices of both types have found applications as identification tags, sensors of different physical quantities, chemical sensors, and biosensors [Pohl, 2000; Seifert at al., 1994; Hribšek et al., 2009; Hribšek et al., 2010; Mitsakakis et al., 2009]. They are used in consumer and highly professional devices and systems. SAW sensors are passive elements (they do not need power supply). The main advantage of all SAW sensors is their ability to be accessed wirelessly enabling remote monitoring in harsh environment. Wireless access is achieved simply by connecting an antenna to the input transducer.

The operation of delay line SAW sensors is based on the fact that the measurand (temperature, pressure, strain, chemical vapour etc.) affects the propagation of the SAW in the sensor in attenuation and delay. If the sensor is heated, stretched or compressed, or if it is mass loaded, the substrate's length and its elasticity constants are changed. These changes cause velocity and phase delay variations, which then proportionally change the centre frequency, attenuation and time delay of the device. The first reported use of SAW technology for a sensor application was in 1975 for pressure sensing [Cullen & Reeder, 1975; Cullen & Montress, 1980]. SAW temperature sensors have millidegree resolution, good

linearity, fast response, and low hysteresis [Pohl, 2000]. They are sealed in hermetic packages. The response time is about 0.3 s, 1000 times faster than in bulk acoustic wave (BAW) sensors. For temperatures up to 200°C lithium niobate is the ideal material for temperature sensors, because of its large temperature coefficient (TCD) of approximately 90 ppm/°C and its high electro-acoustic coupling constant. For temperatures up to 1000°C langasit substrate is used.

SAW chemical vapour sensors were invented by Wohltjen [Wohltjen & Dessy, 1979; Wohltjen, 1982]. A SAW chemical vapour sensor is made from a SAW device by placing chemically sensitive coatings (usually polymer films) on the device surface. The absorbed chemical vapours into the coating cause a change in the centre or resonant frequency of the sensor. A microcomputer can measure these changes and use them to determine the presence and concentration of chemical agents.

The SAW sensor coatings have unique physical properties which allow a reversible adsorption of chemical agents. In order to make the whole system as compact as possible, the SAW device should be incorporated in CMOS or MEMS integrated circuits [Zaki et al., 2006]. In that case piezoelectric material is placed on the top of the IC circuit, e.g. on the top of silicon or the isolating layer, usually silicon dioxide. Commonly used piezoelectric materials in classical SAW applications are ST-cut quartz and lithium niobate. Besides them ZnO, AlGaN, GaN, AlN are used [Zaki et al., 2006; Rufer et al., 2006; Assouar et al., 2000; Rufer et al., 2005; Kirsch et al., 2006; Kirsch et al., 2007; Omori et al., 2008]. Recently, multilayered substrates are used for the wave velocity increase [Ahmadi et al., 2004]. The highest velocities are achieved when the piezoelectric material is placed on the top of the diamond layer, due to its highest acoustic wave velocity [Assouar et al., 2000; Benetti et al., 2004; Benetti et al., 2005; Besmaine et al., 2008; Hakiki et al., 2005; Mortet et al., 2008; Jian et al., 2008; Shikata et al., 2005]. Several piezoelectric materials in combination with diamond/silicon substrates have been investigated theoretically and experimentally.

Theoretical calculation of the wave velocity in the multilayer structures is based on the solution of the wave equation demanding elaborate numerical computations. The use of diamond in the multilayered SAW structure has the following advantages: high frequencies up to 5 GHz, high coupling coefficients up to 1.2%, small temperature deviations, high power capability, and small device size without submicron lithography. The disadvantages of the layered SAW structures are the complex design and the problem related to the deposition of a piezoelectric layer with appropriate crystalline orientation. These facts probably have caused insufficient research on SAW sensors using diamond. Extreme chemical stability and bio-inertness [Specht et al., 2004] make diamond ideal material for sensors operating in harsh or biologic environments.

This chapter describes principles of operation, analyses and modelling of delay line chemical vapour SAW sensors.

2. Principles of chemical vapour SAW sensor operation

The basic principle of chemical vapour SAW sensors is the reversible sorption of chemical vapours by a coating which is sensitive to the vapour to be detected. A transversal, or delay line, SAW chemical sensor can be schematically presented as in Fig. 3. It consists of two IDTs and a chemically sensitive thin layer placed between them on the top surface of the piezoelectric substrate.

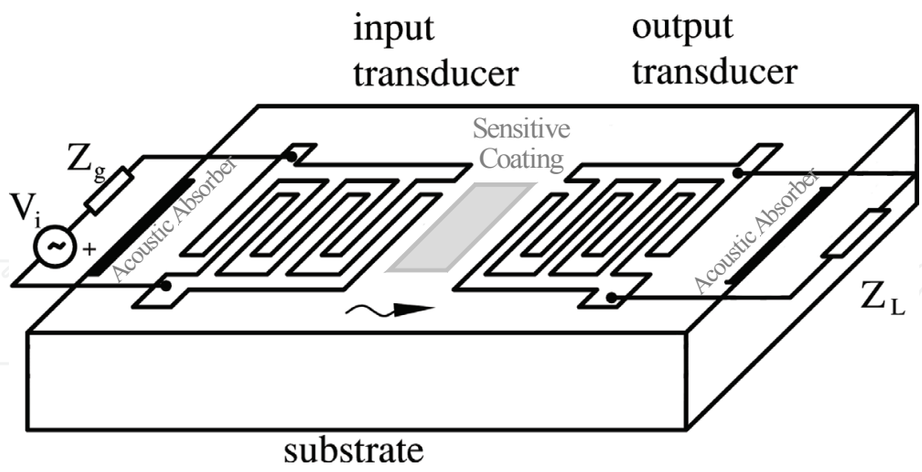

Fig. 3. The basic configuration of a chemical SAW sensor.

The surface wave is induced by an electrical signal applied to the input IDT. The output signal (voltage) is taken from the output IDT. The velocity and attenuation of the wave are sensitive to mass and viscosity of the thin layer, usually polymer film. The purpose of the thin layer is to absorb chemicals of interest. When the chemical is absorbed, the mass of the polymer increases causing a change in velocity and phase of the acoustic signal, which causes a change in amplitude and frequency of the output voltage at the load impedance Z_L. Acoustic absorbers placed on the substrate edges damp unwanted SAW energy and eliminate spurious reflections that could cause signal distortions.

The IDTs are identical with uniformly spaced electrodes of equal lengths and equal ratio of electrodes width and spacing. The number of electrodes defines the frequency bandwidth of a SAW device. The electrodes' lengths and their number, and matching networks at the electrical ports, should be chosen to match the IDT input resistance, at the centre frequency f_0, to the load resistance R_L and the generator resistance R_g. In that case, the overall minimal loss due to IDTs is 12 dB. The wavelength corresponding to the centre frequency equals $2d$ (the distance between the electrodes of the same polarity). The centre frequency and the bandwidth are determined by the IDT`s geometry and the substrate type.

The middle part of a SAW sensor, a delay line, is generally treated as lossless. However, its losses can be neglected only for lower frequencies and small delays (small distances between the transducers). The transfer function of the delay line is normally assumed unity, although this may not be true for high frequencies ($f > 0.5\,\mathrm{GHz}$) or if there are films in the propagation path [Golio, 2008]. In communications, in electrical filtering applications, the distance between the IDTs is small. Quite opposite, in chemical sensors this part is essential and must have a certain length, usually 100–200 wavelengths [Martin et al., 1994], which should be taken into account.

The frequency and the magnitude of the output voltage across the load are proportional to the mass loading of the sensing part. The output voltage in the presence of sensing material (without vapour) serves as a reference. The difference of the output voltage in the presence of vapour and the reference is proportional to the vapour concentration. Sometimes the output voltage is directly measured, but usually a SAW delay line is placed in the feedback loop of the oscillator, Fig. 4, so that the oscillation frequency is proportional to the measurand and it can be easily measured.

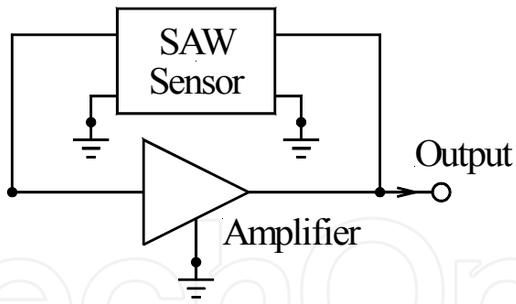

Fig. 4. SAW delay line oscillator.

Time delay τ of the SAW delay line sensor is the ratio of acoustical length L (distance between the first electrodes of the input and output transducers) and SAW velocity v. Generally, in the known sensor applications, L and v are changed due to a temperature change, mechanical stress, and strain, or because of a mass loading from a thin surface layer. In chemical vapour sensors L does not change so that the relative change of the delay due to the variation of a loading from a thin sensitive layer, with or without the vapour, denoted as measurand y, can be expressed as follows:

$$\frac{\mathrm{d}\tau}{\tau} = -\frac{\mathrm{d}v}{v\mathrm{d}y}\mathrm{d}y = \gamma_y \mathrm{d}y \tag{1}$$

where γ_y can be called the delay sensitivity with respect to y. It is determined by the orientation and type of crystalline material used to fabricate the sensor [Pohl, 2000; Živković, 2003].

The oscillations are sustained if the following conditions are met:

- amplification in the open loop is greater than 1,
- net phase in the closed loop, acoustical plus electrical, equals $2n\pi$, where n is the number of the mode, e.g.,:

$$\frac{2\pi fL}{v} + \phi_{\mathrm{A}}(f) = 2\pi n \tag{2}$$

where f is the oscillation frequency, and ϕ_{A} is the phase of the amplifier. Since the electrical delay is much smaller than acoustical, from (1) and (2) can be found:

$$\frac{\mathrm{d}f}{f} = -\frac{\mathrm{d}\tau}{\tau} = -\gamma_y \mathrm{d}y \tag{3}$$

which gives the straight influence of the measurand on the frequency. To avoid temperature influence on measuring results sensors should be made on ST-cut quartz.

In some applications the sensor is a part of a more sophisticated system. In that case two equal SAW sensors are used: one is vapour-free and serves as reference, the other one is exposed to vapour and actually performs the sensing function, Fig. 5. The two SAW sensors are embedded into electrical oscillator circuits and the frequency shift between the oscillators is proportional to the gas concentration. Using an electronic circuit called the mixer the voltage proportional to the vapour concentration is obtained from the frequency shift.

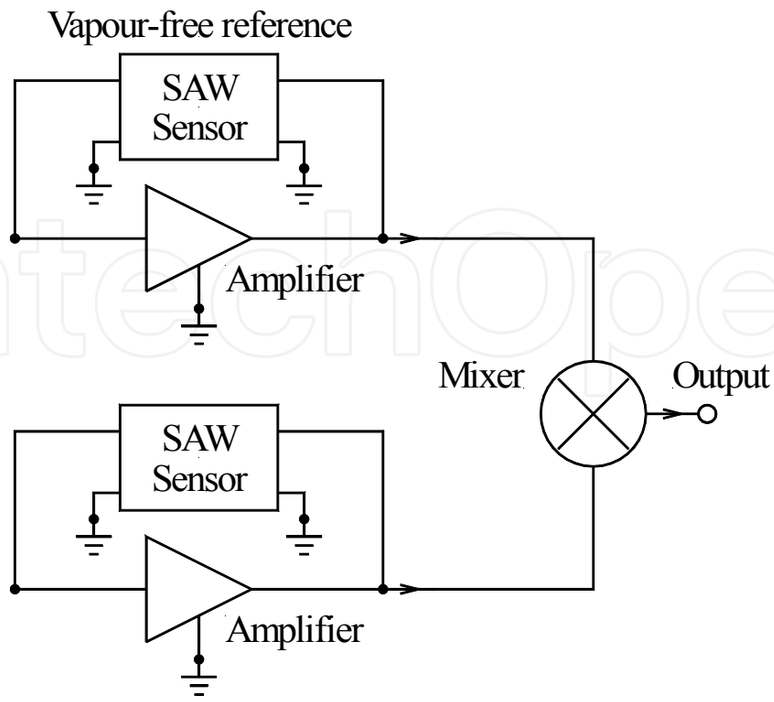

Fig. 5. Block diagram of a differential chemical SAW sensor system.

3. Analyses and modelling of delay line SAW sensors

According to equation (3) the goal of the analysis of SAW chemical sensors is the derivation of formulas which connect the frequency shift and chemical quantities (e.g., vapour concentration). The existing analysis approaches are usually: (a) the analysis based on the wave equation solutions [Wohltjen & Dessy, 1979; Martin et al., 1994], (b) the analysis based on published formulas derived from the wave equation [Grate & Klusty, 1991; Grate & Zellers, 2000], and (c) approximate analysis by means of equivalent electro-mechanical circuits [Živković et al., 2009]. In the first two approaches chemical SAW sensors have been analyzed mainly from the chemical point of view without giving any relations between chemical quantities and the geometry of the SAW sensor and matching conditions at its electrical ports. Only in the last approach the derived formulas give the straightforward connection between the chemical vapour concentration and the geometry of the SAW sensor, sensing part, and substrate properties. The most complete analyses based on the wave equation are reported in [Martin et al., 1994].

In all of these approaches the centre frequency f_0 without sensing film should be known. The centre frequency is proportional to the wave velocity v and inversely proportional to the wavelength λ_0 (which is equal to the period of IDTs $\lambda_0 = 2d$):

$$f_0 = \frac{v}{\lambda_0} \tag{4}$$

If the substrate is single layer piezoelectric crystal the centre frequency can be easily calculated from the IDT geometry and velocity of the material (can be found in the open

literature). However, if the substrate is multilayered, as is the case when the sensor is imbedded in MEMS or integrated circuits or when diamond is used, theoretical velocity determination is rather tedious task and numerical calculation methods are to be performed in each case separately [Mortet et al., 2008; Benetti et al., 2004; Adler et al., 1990].

3.1 Analyses based on wave equation

It is well known that the exact analysis using surface wave theory is very complex even in the case of a free surface and single layer piezoelectric substrate [Farnell, 1977; Martin et al., 1994; Golio, 2008; Ballantine et al., 1997]. It can be found in classical SAW books [Farnell, 1977; Farnell, 1978; Feldman & Henaff, 1989] for single piezoelectric substrate. It starts from the second Newton's law applied to particle motion, which gives a set of partial differential equations. The equations are solved for the appropriate boundary conditions and relations between mechanical and electrical quantities of a piezoelectric substrate. The Maxwell's equations for the electromagnetic field should be taken into account, as well.

Velocity determination is performed by solving wave equations. The wave equations are the partial differential equations of the form [Farnell, 1977; Farnell, 1978; Hribšek, 1982; Hribšek, 1986]:

$$\rho \frac{\partial^2 u_m}{\partial t^2} = \sum_{j=1}^{3} \frac{\partial T_{mj}}{\partial x_j}, \ (m = 1,2,3) \tag{5}$$

where

ρ is the density of the substrate,

u_m is displacement in the direction x_m,

T_{mj} is the component of the stress tensor,

x_j's are space coordinates,

t is time, and

$T_{mn} = T_{nm}$.

Surface wave is propagating in x_1 direction, and x_3 direction is normal to the surface, Fig. 1.

For the piezoelectric substrate the relations between mechanical and electrical variables can be expressed as follows:

$$T_{mn} = c_{mnpq} S_{pq} - e_{pmn} E_p, \ (m,n,p,q = 1,2,3) \tag{6}$$

$$D_m = e_{mnp} S_{np} + \varepsilon_{mn} E_n \tag{7}$$

where

e_{pmn} are the piezoelectric constants of the material (elements of the piezoelectric tensor),

c_{mnpq} are elastic constants of the material measured at the constant electric field,

ε_{mp} are dielectric constants measured at the constant mechanical conditions,

E_p is electric field,

D_m is electric displacement, and

S_{pq} is relative mechanical displacement defined as

$$S_{pq} = S_{qp} = \frac{1}{2}\left(\frac{\partial u_p}{\partial x_q} + \frac{\partial u_q}{\partial x_p} \right). \tag{8}$$

Besides that, Maxwell's equations for electromagnetic field are taken into account. Based on the fact that the electromagnetic field is slowly varying, it can be assumed to be static, e.g., that the electric field is the gradient of a scalar, but variable, potential φ:

$$E_m = -\frac{\partial \varphi}{\partial x_m}. \tag{9}$$

The lack of free charges in the substrate yields

$$\frac{\partial D_m}{\partial x_m} = 0. \tag{10}$$

Using (6)–(10), equations (5) and (10) can be transformed to a more convenient form

$$\rho \frac{\partial^2 u_m}{\partial t^2} - c_{mnpq} \frac{\partial^2 u_p}{\partial x_m \partial x_q} = e_{pmn} \frac{\partial^2 \varphi}{\partial x_p \partial x_m}, \tag{11}$$

$$\varepsilon_{mp} \frac{\partial^2 \varphi}{\partial x_m \partial x_p} = e_{mpq} \frac{\partial^2 u_p}{\partial x_m \partial x_q}. \tag{12}$$

Last equation represents the Laplace equation for anisotropic piezoelectric materials. The equations are solved for the appropriate mechanical and electrical boundary conditions at the surface $x_3 = 0$. For the unloaded surface, the Laplace equation holds for the potential above the surface and

$$T_{3n}\big|_{x_3=0} = 0, \ (n = 1,2,3) \tag{13}$$

Potential and electric displacement D_3 also satisfy the continuity equation for $x_3 = 0$, while for $x_3 = \infty$ vanish. Consequently, potential φ has the form

$$\varphi = \varphi(0) \mathrm{e}^{-kx_3} \mathrm{e}^{\mathrm{j}k(x_1 - vt)} \tag{14}$$

where $k = \omega / v$ is the wave number and v is the wave velocity.
Equations (11) and (12) can be solved only numerically using various methods. One method is to represent the solution as a sum of partial solutions given by [Farnell, 1977; Farnell, 1978]

$$u_m^{(i)} = \alpha_m^{(i)} \mathrm{e}^{\mathrm{j}kb^{(i)}x_3} \mathrm{e}^{\mathrm{j}k(x_1 - vt)}, \ \varphi^{(i)} = u_4^{(i)}, \ (m = 1,2,3,4). \tag{15}$$

Each partial solution must satisfy equations (11)–(12) and equals zero for $x_3 = \infty$. By substituting partial solutions in (11) and (12), a set of four linear algebraic equations is formed in which the coefficients are the functions of density and elastic, dielectric and piezoelectric constants of the substrate. In order to get non trivial solutions, the determinant

of the system must be zero, which gives an algebraic equation of the eighth order (degree) in $b^{(i)}$. Since the wave amplitude decays with substrate's depth, only four solutions within lower halfplane of the complex variable b are of interest. Consequently, the solution has the form

$$u_m = \left(\sum_{i=1}^{4} C_i \alpha_m^{(i)} \, \mathrm{e}^{\mathrm{j}kb^{(i)}x_3} \right) \mathrm{e}^{\mathrm{j}k(x_1 - vt)} \,, \; \varphi = u_4 \,, \; (m = 1,2,3,4) \;. \tag{16}$$

Coefficients k, $b^{(i)}$ and $\alpha^{(i)}$ are the functions of velocity v. Weighting coefficients C_i are found to satisfy boundary conditions at $x_3 = 0$. From these conditions a set of four equations is obtained. Velocity v is calculated setting the determinant of the system to zero. Even in the case of substrate crystals with symmetry, where many of the coefficients c, e and ε are equal to zero, the explicit solution for velocity cannot be found. The solution has to be found numerically, using iterative procedures. When the velocity is calculated, the coefficients C_i can be found, e.g., solutions for the particle motion (displacements) and potential. The procedure can be used for any substrate, but the calculation time depends on the substrate type. From (16) is obvious that all variables are independent of x_2 and u_2. The wave amplitude decays exponentially with the distance from the surface, so that the most of the wave energy is confined within the depth of one wave length. Therefore, the motion in x_1 direction can be generally represented as

$$u_1 = u_1(x_3)\mathrm{e}^{\mathrm{j}\omega t - \gamma x_1} \,, \; \gamma = \alpha + \mathrm{j}k = \alpha + \mathrm{j}\frac{\omega}{v} \tag{17}$$

where

γ is complex propagation factor and

α is attenuation [Ballantine et al., 1997].

For multi layer substrates calculations are even more difficult. In that case, equations (11) and (12), assuming $u_2 = 0$ and that all variables are independent of x_2, expand to three two-dimensional partial differential equations with three unknowns: particle displacement components u_1 and u_3 and potential component ϕ. To find the velocity, these three equations along with two equations for normal stress and one equation for normal electrical displacement are solved in each layer with appropriate boundary conditions at the top and bottom surface and across the interfaces. To find the velocity, matrix techniques can be used [Ahmadi et al., 2004; Adler et al., 1990].

The finite element method (FME) can be also used for multilayer substrates analyses [Sankaranarayanan et al., 2005]. It is employed to calculate the effective phase velocity in multilayer structures with diamond [Hashimoto, 2000; Plessky & Koskela, 2000; Sung et al., 2009].

At McGill University PC Acoustic Wave Software was developed for the velocities calculation in multilayer substrates [Adler et al., 1990].

Derivation of the frequency shift due to the sensing film and chemical quantities can be found from (4):

$$\frac{\Delta f_0}{f_0} = \frac{\Delta v}{v} \,. \tag{18}$$

The velocity shift is not solely determined by the material constants but also by the ratio between the thickness of the piezoelectric layer and the wavelength corresponding to the centre frequency.

Applying perturbation method to the solutions of the wave equation, Tiersten and Sinha derived a formula relating velocity change to film properties for the case of an acoustically thin, elastic film [Tiersten & Sinha, 1978]. Wohltjen first applied the Tiersten formula to analyze the response of polymer-coated SAW sensors [Wohltjen, 1984].

The simplest (and the one most utilized) interaction for SAW sensor applications is the response due to changes in the mass density on the device surface. For that case, in [Ballantine et al., 1997] the relation between the changes in wave velocity, changes in wave energy density, and fractional change in mass density of the lossless medium is derived:

$$\frac{\Delta v}{v_0} = -\frac{\Delta U}{U_0} = -\frac{\Delta \rho}{\rho_0} \tag{19}$$

where v_0, U_0 and ρ_0 denote unperturbed propagation velocity, energy density and density, respectively. Using expression (19), solutions for velocities from the wave equation and grouping together all the substrate-dependent constants, result in the expression for the mass-induced change of the thin film in SAW propagation velocity in the form

$$\frac{\Delta v}{v_0} = -c_m f_0 \rho_s \tag{20}$$

where c_m is the mass sensitivity factor, and ρ_s is the density of the mass load. Coefficient c_m for quartz, lithium niobate and gallium arsenide can be calculated from the data given in [Table 3.1, Ballantine et al., 1997].

In [Martin et al., 1994] a perturbation method is also used to find the changes in the complex propagation factor (velocity and attenuation) contributed by acoustically thin and thick visco-elastic polymer films. In acoustically thin films, displacement is uniform across the film and varies only in the direction of propagation. For thick films, inertial effects cause a phase lag across the film for shear displacements. To obtain velocity changes linearly proportional to absorbed vapour concentration, it is necessary that the film remains in the acoustically thin regime [Martin et al., 1994]. The regime of the film operation can be determined from the ratio R of cross-film to in-plane gradients induced by the SAW [Martin et al., 1994]:

$$R = \frac{A f v_0 \rho h}{|G|} \tag{21}$$

where

ρ, h and G are the film density, thickness, and shear modulus, respectively;

A is a substrate-dependent parameter (having a value of 1.9 for ST-cut quartz) [Martin et al., 1994].

When the film coating is sufficiently thin (small h) and rigid (large G) such that $R << 1$, the film is *acoustically thin*. If the film properties are such that $R >> 1$, the film is *acoustically thick*.

When the films are elastic the intrinsic elastic moduli are real, resulting in zero attenuation changes, and the Tiersten formula [Tiersten & Sinha, 1978] for fractional velocity change, written in terms of the Lamé constants (λ, μ) [Martin et al., 1994; Ballantine et al., 1997]:

$$\frac{\Delta v}{v_0} = -\omega h\left(c_1\left(\rho - \frac{\mu}{v_0^2}\right) + c_2\rho + c_3\left(\rho - \frac{4\mu}{v_0^2}\frac{\lambda+\mu}{\lambda+2\mu}\right)\right) \tag{22}$$

Where ω is the angular frequency and c_i are the elastic constants of the material.
Wohltjen described the frequency shift Δf_s due to a thin, non-conducting film as [Wohltjen, 1984]

$$\Delta f_s = (k_1 + k_2)F^2 h\rho - k_2 F^2 h(4\mu / V_R^2)[(\lambda+\mu)/\lambda+2\mu)] \tag{23}$$

where
F is the centre frequency of a SAW device,
V_R is the wave velocity in the substrate, and
k_1, k_2 are material constants of the substrate. If only mass loading is taken into account, frequency shift is calculated using the first term in (23).
In [Grate et al., 1988; Grate et al., 1992] frequency shift Δf_v due the vapour sorbed in the film is given by

$$\Delta f_v = \frac{\Delta f_s C_v K}{\rho} \tag{24}$$

where
C_v is the concentration of the vapour in the vapour phase, and
K is the partition coefficient, which is the ratio of the concentration of the vapour in the sorbent phase, C_s, to the concentration of the vapour in the gas phase, C_v.
In [Grate & Zellers, 2000] equation (24) is modified to include the contribution of swelling-induced modulus changes to vapour sensor responses:

$$\Delta f_v = \frac{\Delta f_s C_v K}{\rho_s} + f_L \frac{C_v K}{\rho_L}\frac{\Delta f_s A_{SAW}}{\alpha} \tag{24a}$$

$$\Delta f_v = \frac{\Delta f_s C_v K}{\rho_s} + f_1 v_1 \frac{\Delta f_s A_{SAW}}{\alpha} \tag{24b}$$

3.2 Analysis based on published formulas

Typically, the published formulas which connect frequency shifts and chemical compounds quantities are applied formally, without any insight into the influence of many properties of a real SAW delay line (geometry, propagation losses, technological constraints, and production tolerances) on the frequency change. This is the reason why some researchers perform more experiments than needed, or have difficulties in explaining discrepancies between the expected and measured values [Joo et al., 2005]. The mostly used formula for the frequency shift is actually equation (20) expressed in a slightly different form. In [Balcerzak & Zhavnerko, 2007] it has the form (neglecting the changes of viscoelasticity, dielectric constant and electric conductivity of the layer)

$$\Delta f = K_s f_0^2 \Delta m \frac{1}{A} \tag{25}$$

where

K_s is a constant (for lithium niobate $K_s = 5.49 \cdot 10^{-11}\,\mathrm{s\,m^2 g^{-1}}$),

f_0 is operating frequency of the sensor,

A is the surface of chemosensitive layer, and

Δm is the change of mass bonded to the sensor.

In [Benetti et al., 2004] it is in the form

$$\Delta f = -c_m f_0^2 h' \Delta \rho_s \tag{26}$$

where

c_m is the mass sensitivity coefficient (frequency independent),

h' is the thickness of the part of the coating that incorporates gas molecules, and

$\Delta \rho_s$ is the mass density change due to absorption.

In [Ho et al., 2003] modifications of (24) are used.

3.3 Analyses based on the electro-mechanical equivalent circuit

The analysis of transversal chemical SAW sensors, based on the electro-mechanical equivalent circuit, develops in a straight forward manner explicit general relations between electrical signals, voltages or frequencies, and vapour detection estimations taking into account properties of real SAW devices [Živković et al., 2009]. The whole sensor is modelled as a two-port network consisting of three parts: (1) the input interdigital transducer, (2) the delay line that is the sensing part, and (3) the output interdigital transducer, Fig. 6. The transducers are modelled as three-port networks and the delay line as a two-port network. The closed form formula for vapour concentration estimation is derived using analogy between electrical and mechanical quantities, the properties of the surface wave and the technological process and implementation of the sensor.

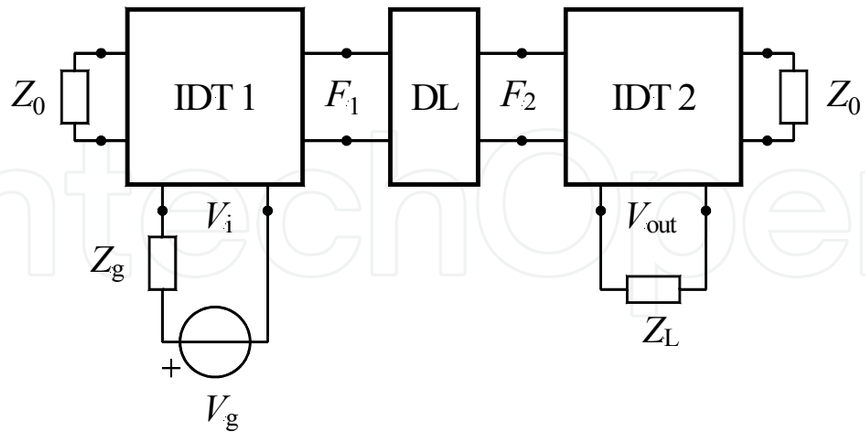

Fig. 6. The equivalent circuit of a SAW sensor.

The characteristic SAW acoustic impedance of the unloaded substrate is designated by Z_0 and the acoustic impedance due to the mass loading of the thin film is Z_m :

$$Z_0 = A \rho_s v \tag{27}$$

$$Z_{\mathrm{m}} = A_{\mathrm{m}} \rho_{\mathrm{m}} v \tag{28}$$

where

A is the substrate cross-section area through which the waves propagate,

ρ_{s} is the mass density of the piezoelectric substrate,

v is the SAW velocity in the piezoelectric substrate,

A_{m} is the cross-section area of the thin film, and

ρ_{m} is the mass density of the film.

$Z_{\mathrm{g}} = R_{\mathrm{g}}$ and $Z_{\mathrm{L}} = R_{\mathrm{L}}$ are purely resistive electrical impedances of the generator and the electrical load, respectively.

The relative variation of the centre frequency due to the mass loading is equal to the relative variation of the wave velocity, equation (18), and can be found using the equivalent circuit of a mass loaded delay line, Fig. 7.

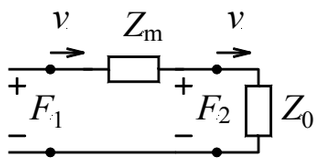

Fig. 7. The equivalent circuit of a mass loaded delay line.

By analogy between electrical and mechanical quantities, the relative variation of frequency and the relative variation of velocity, for Z_{m} much smaller than Z_0, are

$$\frac{\Delta f}{f_0} = \frac{\Delta v}{v} = \frac{-Z_{\mathrm{m}}}{Z_0} = \frac{-\rho_{\mathrm{m}} h_{\mathrm{m}}}{\rho_{\mathrm{s}} \lambda_0} K_{\mathrm{w}} \tag{29}$$

where

ρ_{m} and h_{m} are the density and thickness of the thin layer, respectively,

ρ_{s} is the density of the piezoelectric substrate, and

K_{w} is a coefficient that depends on the technological process and implementation of the sensor.

The components of the wave decay exponentially inside the substrate and the penetration is of the order of one wavelength. Therefore, in (29), instead of the substrate thickness, one wavelength λ_0 is used. From the last equation Δf can be determined as

$$\Delta f = -\frac{\rho_{\mathrm{m}} h_{\mathrm{m}}}{\rho_{\mathrm{s}} v} f_0^2 K_{\mathrm{w}} \tag{30}$$

The last equation shows that the higher sensitivity will be obtained if the centre frequency is higher, thickness and density of the film larger, and the substrate density and velocity smaller. This means that quartz ($\rho_{\mathrm{s}} = 2.62\ \mathrm{g/cm^3}$) is a better choice for the substrate than lithiumniobate ($\rho_{\mathrm{s}} = 4.7\ \mathrm{g/cm^3}$). Furthermore, if ST-cut quartz is used temperature dependence can be neglected. Using the last equation the frequency shift, Δf_{p}, due to the sensing film (without vapour) can be determined:

$$-\frac{\Delta f_{\mathrm{p}}}{f_0} = \frac{\rho_{\mathrm{p}} h_{\mathrm{p}}}{\rho_{\mathrm{s}} v} f_0 K_{\mathrm{w}} \tag{31}$$

where ρ_p and h_p are the density and thickness of the film, respectively.
Using the same reasoning, the fact that h_p is much smaller than λ_0, and the partition coefficient K, the frequency shift Δf_{vap} due to the concentration of the vapour in the vapour phase C_v (concentration in the ambient), can be calculated as:

$$\Delta f_{vap} = KC_v \frac{\Delta f_p}{\rho_p} \tag{32}$$

4. Conclusion

Analysis of chemical SAW sensors can be approached to in three ways: (1) exact analysis by solving the wave equation, (2) published formulas which connect frequency shifts and chemical compounds quantities, and (3) approximate analysis by means of equivalent electro-mechanical circuits.
The exact analysis of SAW sensors using surface wave theory is very complex even in the case of a free surface of a single layer piezoelectric substrate.
The published formulas which connect frequency shifts and chemical compounds quantities are applied formally, without any insight into the influence of many properties of a real SAW delay line (geometry, propagation losses, technological constraints, and production tolerances) on the frequency change. This is the reason why some researchers perform more experiments than needed, or have difficulties in explaining discrepancies between the expected and measured values.
The analysis based on electro-mechanical equivalent circuits of SAW sensors connects, in a straight forward manner, electrical signals and chemical vapour concentrations, taking into account important properties of real SAW devices, such as propagation losses, technological constraints, and production tolerances. The unique feature of this approach is a set of closed form analytic expressions for vapour concentration estimations. The expressions explicitly relate the vapour concentration, substrate parameters, and centre frequency. They enable insight into the influence of the sensor design parameters on the sensor performance and predict very efficiently and correctly the frequency and voltage shifts due to the vapour concentrations. The closed-form expressions can be used for the design of optimal sensors for a given vapour.

5. References

Adler, E. L.; Slaboszewicz, J. K.; Farnell, G. W. & Jen, C. K. (1990). PC software for SAW propagation in anisotropic multilayers, *IEEE Transactions on Ultrasonics, Ferroelectrics, and Frequency Control*, Vol. 37, No. 3, May 1990, pp. 215-223, ISSN 0885-3010.

Ahmadi, S.; Hassani, F.; Korman, C.; Rahaman, M. & Zahloul M. (2004). Characterization of Multy- and Single- layer Structure SAW Sensor, *Proceedings of the IEEE Conference on Sensors*, pp. 1129–1132, Vienna, Austria, Oct. 24–27, 2004.

Assouar, M. B.; Elmazria, O.; Jimenez, R.; Sarry, F. & Alnot, P. (2000). Modelling of SAW filter based on ZnO/diamond/Si layered structure including velocity dispersion, *Applied Surface Science*, Vol. 164, No. 1-4, Sept. 2000, pp. 200–204, ISSN 0169-4332.

Ballantine, D. S.; White, R. M.; Martin, S. J.; Ricco, A. J.; Zellers, E. T.; Frye, G. C.; Wohltjen, H. (1997). *Acoustic Wave Sensors: Theory, Design, Physico-Chemical Applications*, Academic Press, ISBN 0-12-077460-7, San Diego, USA.

Balcerzak, A. & Zhavnerko, G. (2007). Ultrasonic Chemical Sensor For Detection of Vapors of Some Volatile Organic Compounds, *Molecular and Quantum Acoustics*, Vol. 28, 2007, pp. 7-12.

Benetti, M.; Cannata, D.; D'Amico, A.; Di Pietrantonio, F.; Macagnano, A. & Verona, E. (2004). SAW Sensors on AlN/Diammond/Si Structures, *Proceedings of the IEEE Conference on Sensors*, pp. 753–756, Vienna, Austria, Oct. 24–27, 2004.

Benetti, M.; Cannatta, D.; Pietrantonio, F. D. & Verona, E. (2005). Growth of AlN piezoelectric film on diamond for high-frequency surface acoustic wave devices, *IEEE Transactions on Ultrasonics, Ferroelectrics, and Frequency Control*, Vol. 52, No. 10, 2005, pp. 1806–1811, ISSN 0885-3010.

Besmaine, S.; Brizoual, L. Le; Elmazria, M.; Fundenberger, J. J.; Belmahi, M. & Benyoucef, B. (2008). SAW devices based on ZnO inclined c-axis on diamond, *Diamond and Related Materials*, Vol. 17, No. 7-10, 2008, pp. 1420-1423, ISSN 0925-9635.

Comini, G.; Faglia, G. & Sberveglieri X. (2009). *Solid State Gas Sensing*, Springer Science+Business Media LLC, ISBN 0387096647, New York, USA.

Cullen, D. & Reeder, T. (1975). Measurement of SAW Velocity Versus Strain for YX and ST Quartz, *Proceedings of Ultrasonics Symposium*, pp. 519-522, Sept. 1975.

Cullen, D. & Montress, T. (1980). Progress in the Development of SAW Resonator Pressure Transducers, *Proceedings of Ultrasonics Symposium*, Vol. 2, pp. 696-701, Nov. 1980.

Data Sheet-07-2093/September (2005). MSA International, ©MSA 2005, http://www.MSAnet.com

Farnell, G. W. (1977). Elastic Surface Waves, In *Surface Wave Filters*, Matthews, H. (Ed.), pp. 1-55, John Wiley, ISBN 0471580309, New York, USA.

Farnell, G. W. (1978). Types, Properties of Surface Waves, In *Acoustic Surface Waves*, Oliner, A. A. (Ed.), Springer Verlag, ISBN 0387085750, Germany.

Feldman, M. & Henaff, J. (1989). *Surface acoustic waves for signal processing*, Artech House, ISBN 0890063087, London, UK.

Golio, M. (2008). *The RF and Microwave Handbook*, 2nd Ed., CRC Press LLC, ISBN 0849372178, Boca Raton, USA.

Grate, J. W.; Snow, A.; Ballantine, D. S.; Wohltjen, H.; Abraham, M. H.; McGill, R. A. & Sasson, P. (1988). Determination of partition coefficients from surface acoustic wave vapor sensor responses and correlation with gas-liquid chromatographic partition coefficients, *Analytical Chemistry*, Vol. 60, No. 9, May 1988, pp. 869-875, ISSN 0003-2700.

Grate, J. W. & Klusty, M. (1991). Surface Acoustic Wave Vapor Sensor Based on Resonator Devices, *NRL Memorandum report 6829*, May 23, 1991, pp. 1-38.

Grate, J. W.; Klusty, M.; McGill, R. A.; Abraham, M. H.; Whiting, G. & Andonian-Haftvan, J. (1992). The predominant role of swelling-induced modulus changes of the sorbent phase in determining the responses of polymer-coated surface acoustic-wave vapor sensors, *Analytical Chemistry*, Vol. 64, No. 6, March 1992, pp. 610-624, ISSN 0003-2700.

Grate, J. W. & Zellers, E. T. (2000). The Fractional Free Volume of the Sorbed Vapor in Modeling the Viscoelastic Contribution to Polymer-Coated Surface Acoustic Wave Vapor Sensor Responses, *Analytical Chemistry*, Vol. 72, No. 13, July 2000, pp. 2861-2868, ISSN 0003-2700.

Hakiki, El; Elmazria, M.; Assouar, O.; Mortet, M. B.; Brizoual, V. Le; Vanecek, L. & Alnot, M. (2005). ZnO AlN diamond layered structure for SAW devices combining high velocity and high electromechanical coupling coefficient, *Diamond & Related Materials*, Vol. 14, No, 3-7, 2005, pp. 1175-1178, ISSN 0925-9635.

Hashimoto, K. Y. (2000). *Surface Acoustic Wave Devices in Telecommunications: Modeling and Simulation*, Springer, ISBN 354067232X, USA.

Ho, C. K.; Lindgren, E. R.; Rawlinson, K. S.; McGrath, L. K.; Wright, J. L. (2003). Development of a Surface Acoustic Wave Sensor for In-Situ Monitoring of Volatile Organic Compounds, *Sensors*, Vol. 3, No. 7, July 2003, pp. 236-247, ISSN 1424-8220.

Hribšek M. (1982). Elementi sa površinskim akustičnim talasom i njihova primena, *Tehnika-Elektrotehnika*, Vol. 31, 1982, pp. 1725-1733. (survey paper) in Serbian

Hribšek M. (1986). Surface Acoustic Wave Devices and their applications, *Proceedings of MIEL'86*, Vol. 1, pp. 37-46, Belgrade, Serbia, 1986. (invited paper)

Hribšek, M.; Ristić, S.; Živković, Z. & Tošić, D. (2009). Modelling of SAW Biosensors, *Proceedings of the International Conference on Biomedical Electronics and Devices (BIODEVICES 2009)*, pp. 376-379, ISBN 978-989-8111-64-7, Porto, Portugal, Jan. 14-17, 2009, INSTICC Press.

Hribšek M.; Tošić D. & Radosavljević M. (2010). Surface Acoustic Wave Sensors in Mechanical Engineering, *FME Transactions*, Vol. 38, No. 1, 2010, pp. 11-18, ISSN 1451-2092.

Hribšek M. F.; Ristić S. S. & Radojković B. M. (2010). Diamond in Surface acoustic wave sensors, *Acta Physica Polonica A*, Vol. 117, No. 5, May 2010, pp. 794-798, ISSN 1898-794X.

Jian, S.; YiZhen, B.; JingChang, S.; GuoTong, D. & Xin, J. (2008). Structural and electrical properties of ZnO films on freestanding thick diamond films, *Chinese Science Bulletin*, Vol. 53, No. 19, Oct. 2008, pp. 2931-2934, ISSN 1001-6538.

Joo, B.-S.; Lee, J.-H.; Lee, E.-W.; Song, K.-D. & Lee, D.-D. (2005). Polymer Film SAW Sensors for Chemical Agent Detection, *Proceedings of the 1st International Conference on Sensing Technology*, pp. 307-310, Palmerston North, New Zealand, Nov. 21-23, 2005

Kannan, O. K.; Bhalla, R.; Kapoor, J. C.; Nimal, A. T.; Mittal, U. & Yadava, R.D.S. (2004). Detection of Landmine Signature using SAW-based Polymer-coated Chemical Sensor, *Defence Science Journal*, Vol. 54, No. 3, July, 2004, pp. 309-315, ISSN 0011748X.

Kirsch, P.; Assouar, M. B.; Elmazria, O.; Mortet, V. & Alnot, P. (2006). GHz surface acoustic wave devices based on aluminum nitride/diamond layered structure realized using electron beam lithography, *Appl. Phys. Letts.*, Vol. 88, No. 22, 2006, 223504/1-3 doi:10.1063/1.2208372

Kirsch, P.; Assouar, M. B.; Elmazria, O.; Hakiki, M. E.; Moret, V. & Alnot, P. (2007). Combination of e-beam lithography and of high velocity AlN/diamond-layered structure for SAW filters in X-band, *IEEE Transactions on Ultrasonics, Ferroelectrics, and Frequency Control*, Vol. 54, 2007, pp. 1486–1491, ISSN 0885-3010.

Martin, S. J.; Frye, G. C. & Senturia, S. D. (1994). Dynamics and Response of Polymer-Coated Surface Acoustic Wave Devices: Effect of Viscoelastic Properties and Film Resonance. *Analytical Chemistry*, Vol. 66, 1994, pp. 2201-2219, ISSN 0003-2700.

Mitsakakis, K. et al. (2009). SAW device integrated with microfluidics for array-type biosensing, *Microelectronics Engineering*, 2009, doi:10.1016/j.mee.2008.12.063

Mortet, V.; Williams, O. A. & Haenen, K. (2008). Diamond: a material for acoustic devices, *p hys. stat. sol. (a)*, 205, No. 5, 1009–1020, DOI 10.1002/pssa.200777502

Omori, T.; Kobayashi, A.; Takagi, Y.; Hashimoto, K. & Yamaguchi, M. (2008). Fabrication of SHF range SAW devices on AlN/Diamond-substrate, *Proceedings of Ultrasonics Symposium*, pp. 196–200, Nov. 2-5, 2008

Plessky, V. & Koskela, J. (2000). "Coupling-of-modes analysis of SAW devices,"International Journal of High Speed Electronics and Systems, vol. 10, pp. 867–947.

Pohl A. (2000). A Review of Wireless SAW Sensors. *IEEE Transactions on Ultrasonics, Ferroelectrics, and Frequency Control*, Vol. 47, 2000, pp. 317-332, ISSN 0885-3010.

Rayleigh, L. (1885). On waves propagated along the plane surface of an elastic solid, *Proc. London Math. Soc.*, Vol. 17, 1885, 4-11.

Rufer, L.; Torres, A.; Mir, S.; Alam, M. O.; Lalinsky, T.; Chan, Y. C. (2005). SAW chemical sensors based on AlGaN/GaN piezoelectric material system: acoustic design and packaging considerations, *Proceedings of the 7th International Conference on Electronics Materials and Packaging, EMAP 2005*, pp. 204-208, 2005, Tokyo, Japan.

Rufer, L.; Lalinský, T.; Grobelný, D.; Mir, S.; Vanko, G.; Őszi, Zs.; Mozolová, Ž. & Gregus, J. (2006). GaAs and GaN based SAW chemical sensors: acoustic part design and technology, *Proceedings of the 6th International Conference on Advanced Semiconductor Devices and Microsystems, ASDAM 2006*, pp. 165-168, 2006, Smolenice, Slovakia.

Sankaranarayanan, S.; Bhethanabotla, V. R. & Joseph, B. (2005). A 3-D Finite Element Model of Surface Acoustic Wave Sensor Response, *Proceedings of the 208th ECS Meeting, Acoustic Wave Based Sensors and Sensor Systems*, Vol 1, Issue 19, pp. 19-27, ISBN 978-156-677-493-2, Los Angeles, California, October 16-21, 2005, Curran Associates, Inc.

Seifert, F.; Bulst, W.E. & Ruppel, C. (1994). Mechanical sensors based on surface acoustic waves, *Sensors and Actuators A*, Vol. 44, No. 3, 1994, pp. 231-239, ISSN 0924-4247.

Shikata, S.; Fujii, S.; Uemura, T.; Itakura, K.; Hachigo, A.; Kitabayashi, H.; Nakahata, H. & Takada, Y. (2005). Improvements of diamond SAW device characteristic and applications to communication system, *New Diamond and Frontier Carbon Tehnology*, Vol. 15, No. 6, 2005, pp. 350-361, ISSN 1334-9931.

Specht, C. G.; Williams, O. A.; Jackman, R. B. & Schoepfer, R. (2004). Ordered growth of neurons on diamond, *Biomaterials*, Vol. 25, No. 8, Aug. 2004, pp. 4073- 4078, ISSN 0142-9612.

Sung, C.-C.; Chiang, Y.-F.; Ro, R.; Lee, R. & Wu, S. (2009). Theoretical analysis of SAW propagation characteristics in (100) oriented AlN/diamond structure, *Proceedings of the Frequency Control Symposium 2009 Joint with the 22nd European Frequency and Time forum*, *IEEE International*, pp. 446-449, ISSN 1075-6787, Besancon, April 2009.

Tiersten, H. F. & Sinha, B. K. (1978). A perturbation analysis of the attenuation and dispersion of surface waves, *Journal of Applied Physics*, Vol. 49, No. 1, Jan 1978, pp. 87-95, ISSN 0021-8979.

White, R. M. & Voltmer, F. W. (1965). Direct Piezoelectric Coupling to Surface Electric Waves, Applied Physical Letters, Vol. 7, No. 12, Dec. 1965, pp. 314-316, ISSN 0003-6951.

Wohltjen, H.; Dessy, R. (1979). Surface acoustic wave probe for chemical analysis. I. Introduction and instrument description, *Analytical Chemistry*, Vol. 51, No. 9, Aug. 1979, pp. 1458-1464, ISSN 0003-2700.

Wohltjen, H. (1982). US. Patent 4,312,228, Jan. 26, 1982.

Wohltjen, H. (1984). Mechanism of operation and design considerations for surface acoustic wave device vapour sensors, *Sensors and Actuators*, Vol. 5, No. 4, July 1984, pp. 307-325, ISSN 0924-4247.

Zaki, A.; Elsimary, H. & Zaghloul, M. (2006). Miniature SAW Device for RF-Wireless Applications Using MEMS Technology, *Proceedings of the 5th WSEAS International Conference on Circuits, Systems, Electronics Control and Signal Processing*, pp.10–13, ISBN ~ ISSN 1790-5117, 960-8457-55-6, Dallas, USA, Nov. 1–3, 2006, World Scientific and Engineering Academy and Society (WSEAS), Stevens Point, Wisconsin, USA.

Živković, Z. (2003). SAW sensors and their applications, *Proceedings of XLVII ETRAN*, Vol. III, pp. 424-427, Herceg Novi, Monte Negro, June 2003. (in Serbian)

Živković, Z.; Hribšek, M. & Tošić, D. (2009). Modeling of Surface Acoustic Wave Chemical Vapor Sensors, *Journal of Microelectronics, Electronic Components, Materials*, Vol. 39, No. 2, June 2009, pp.111-117, ISSN 0352-9045.

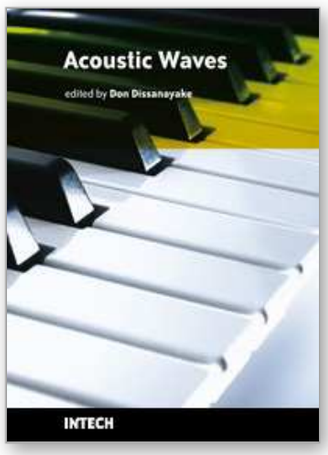

Acoustic Waves
Edited by Don Dissanayake

ISBN 978-953-307-111-4
Hard cover, 434 pages
Publisher Sciyo
Published online 28, September, 2010
Published in print edition September, 2010

SAW devices are widely used in multitude of device concepts mainly in MEMS and communication electronics. As such, SAW based micro sensors, actuators and communication electronic devices are well known applications of SAW technology. For example, SAW based passive micro sensors are capable of measuring physical properties such as temperature, pressure, variation in chemical properties, and SAW based communication devices perform a range of signal processing functions, such as delay lines, filters, resonators, pulse compressors, and convolvers. In recent decades, SAW based low-powered actuators and microfluidic devices have significantly added a new dimension to SAW technology. This book consists of 20 exciting chapters composed by researchers and engineers active in the field of SAW technology, biomedical and other related engineering disciplines. The topics range from basic SAW theory, materials and phenomena to advanced applications such as sensors actuators, and communication systems. As such, in addition to theoretical analysis and numerical modelling such as Finite Element Modelling (FEM) and Finite Difference Methods (FDM) of SAW devices, SAW based actuators and micro motors, and SAW based micro sensors are some of the exciting applications presented in this book. This collection of up-to-date information and research outcomes on SAW technology will be of great interest, not only to all those working in SAW based technology, but also to many more who stand to benefit from an insight into the rich opportunities that this technology has to offer, especially to develop advanced, low-powered biomedical implants and passive communication devices.

Phone: +385 (51) 770 447
Fax: +385 (51) 686 166
www.intechopen.com

Phone: +86-21-62489820
Fax: +86-21-62489821

IntechOpen

IntechOpen